

Constraining the Radii of Neutron Stars with Terrestrial Nuclear Laboratory Data

Bao-An Li¹ and Andrew W. Steiner²

¹*Department of Chemistry and Physics, P.O. Box 419,*

Arkansas State University, State University, Arkansas 72467-0419, USA

²*Theoretical Division, Los Alamos National Laboratory, Los Alamos, NM 87545, USA*

(Dated: April 24, 2019)

Neutron star radii are primarily determined by the pressure of isospin asymmetric matter which is proportional to the slope of the nuclear symmetry energy. Available terrestrial laboratory data on the isospin diffusion in heavy-ion reactions at intermediate energies and studies of the size of neutron skin in ^{208}Pb constrain the slope of the symmetry energy. Using this constraint, we show that the radius (radiation radius) of a 1.4 solar mass (M_{\odot}) neutron star is between 11.5 (14.4) and 13.6 (16.3) km. The available laboratory data also indicates that the direct URCA process will occur in neutron stars with masses larger than about 1.39 solar masses.

PACS numbers: 25.70.-z, 26.60.+c, 97.60.Jd, 24.10.-i

With central pressures of 10^{36} dynes/cm² and gravitational binding energies of 10^{53} ergs, neutron stars are among the most exotic objects in the universe. Impressive progress has been made on the observable properties of neutron stars, such as masses, radii, spectra, and rotational properties [1, 2, 3, 4, 5, 6, 7]. However, a precise neutron star radius measurement still eludes us.

The theoretical understanding of these observable properties demands an understanding of the relevant nuclear physics. For recent reviews, see Refs. [8, 9, 10, 11, 12]. The global properties of neutron stars: masses, radii, and composition, are determined by the Equation of State (EOS) of neutron-rich nucleonic matter, thus neutron stars are ideal astrophysical laboratories for investigating the EOS. The EOS can be separated into two contributions, the isospin symmetric part (the EOS of nuclear matter, E_{nuc}) and the isospin asymmetric part (the nuclear symmetry energy, E_{sym}). This separation is manifest in the relation $E(\rho, \delta) = E_{\text{nuc}}(\rho) + \delta^2 E_{\text{sym}}(\rho)$, where ρ is the baryon density, $\delta = (\rho_n - \rho_p)/\rho$ is the isospin asymmetry, and ρ_n and ρ_p are the neutron and proton densities. While many neutron star properties depend on both parts of the equation of state, the radius is primarily determined by the slope of the symmetry energy, $E'_{\text{sym}}(\rho)$ [8]. Thus knowledge about the symmetry energy from terrestrial experiments will allow us to predict the radius of neutron stars or vice versa.

Recent efforts in terrestrial nuclear laboratories have led to constraints on the EOS of neutron-rich matter, see, e.g., Refs. [13, 14, 15, 16] for reviews. In particular, some significant progress has been made recently in determining the density dependence of $E_{\text{sym}}(\rho)$: (i) isospin diffusion in heavy-ion reactions at intermediate energies is a very sensitive probe of the $E_{\text{sym}}(\rho)$ around the saturation density [17, 18, 19, 20, 21, 22], (ii) flow in heavy-ion collisions at higher energies has constrained the equation of state of nuclear matter [15], and (iii) the sizes of neutron skins in heavy nuclei are sensitive to the $E_{\text{sym}}(\rho)$ at sub-saturation densities [12, 23, 24].

The observational determination of a neutron star radius from the measured spectral fluxes relies on a nu-

merical model of the neutron star atmosphere and uses the composition of the atmosphere, a measurement of the distance, the column density of x-ray absorbing material, and the surface gravitational redshift as inputs. Many of these quantities are difficult to measure, thus the paucity of radius measurements. Current estimates obtained from recent x-ray observations have given a wide range of results.

In this Letter, we combine recently obtained isospin diffusion data, information from flow observables, studies on the neutron skin of ^{208}Pb , and other information to constrain the radius of 1.4 M_{\odot} neutron stars.

We use the EOS corresponding to the single nucleon potential [25, 26]

$$\begin{aligned} U(\rho, \delta, \vec{p}, \tau, x) = & A_u(x) \frac{\rho_{\tau'}}{\rho_0} + A_l(x) \frac{\rho_{\tau}}{\rho_0} \\ & + B \left(\frac{\rho}{\rho_0} \right)^{\sigma} (1 - x\delta^2) - 8\tau x \frac{B}{\sigma+1} \frac{\rho^{\sigma-1}}{\rho_0^{\sigma}} \delta \rho_{\tau'} \\ & + \frac{2C_{\tau, \tau}}{\rho_0} \int d^3 p' \frac{f_{\tau}(\vec{r}, \vec{p}')} {1 + (\vec{p} - \vec{p}')^2 / \Lambda^2} \\ & + \frac{2C_{\tau, \tau'}}{\rho_0} \int d^3 p' \frac{f_{\tau'}(\vec{r}, \vec{p}')} {1 + (\vec{p} - \vec{p}')^2 / \Lambda^2}. \end{aligned} \quad (1)$$

Here $\tau = 1/2$ ($-1/2$) for neutrons (protons) with $\tau \neq \tau'$, $\sigma = 4/3$, and $f_{\tau}(\vec{r}, \vec{p})$ is the phase space distribution function. The incompressibility K_0 of symmetric nuclear matter at ρ_0 is set to be 211 MeV. Eq. 1 is an extension of the well-known MDYI potential of Welke et al. [27] from symmetric to asymmetric matter. The parameter x was introduced to mimic various predictions on $E_{\text{sym}}(\rho)$ by using different many-body theories and effective interactions. The $A_u(x)$ and $A_l(x)$ depend on the x parameter according to $A_u(x) = -95.98 - x \frac{2B}{\sigma+1}$, and $A_l(x) = -120.57 + x \frac{2B}{\sigma+1}$ such that the same saturation properties of symmetric matter and a value of $E_{\text{sym}}(\rho_0) = 32$ MeV are always obtained.

The isoscalar potential estimated from $(U_{\text{neutron}} + U_{\text{proton}})/2$ agrees very well with predictions from variational many-body theory [28]. The underlying EOS has

been tested successfully against nuclear collective flow data in relativistic heavy-ion reactions [15, 27, 29] for densities up to five times saturation density. Also, the strength of the momentum-dependent isovector potential at ρ_0 estimated from $(U_{neutron} - U_{proton})/2\delta$ agrees very well with the Lane potential extracted from nucleon-nucleus scatterings and (p,n) charge exchange reactions with beam energies up to about 100 MeV [26, 30].

We focus on the properties of spherically-symmetric, non-rotating, non-magnetized neutron stars at zero temperature by solving the Tolman-Oppenheimer-Volkov equation. For the equation of state below about 0.07 fm⁻³, we use the results from Refs. [31, 32]. Also, we assume that the neutron star consists of $npe\mu$ matter, but does not contain any exotic components, such as hyperon, quarks, or Bose condensates.

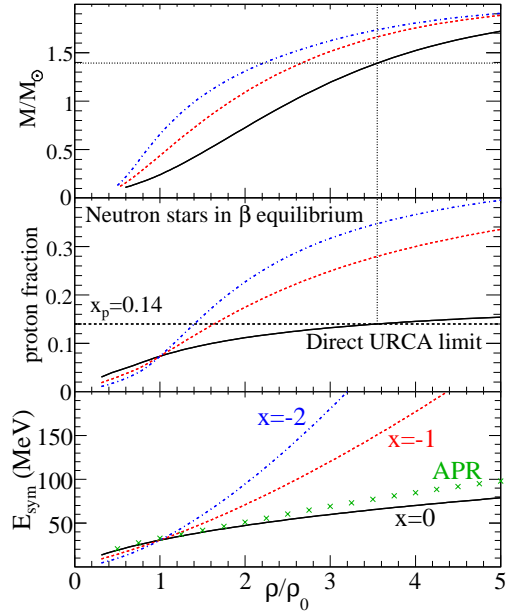


FIG. 1: (Color online) Neutron star mass as a function of the central density, and the proton fraction for beta-equilibrated matter and symmetry energy as a function of density for the EOS with $x = 0, -1$, and -2 . The crosses marked APR give the symmetry energy for the APR EOS.

In Fig. 1 we display some of the basic properties of the EOS and the corresponding neutron stars. Shown in the lower panel is the symmetry energy for $x = 0, -1$ and -2 , respectively. With $x = 0$ the symmetry energy agrees very well with the prediction from Akmal, et. al. (APR) [33] up to about $5\rho_0$. Around ρ_0 , the $x = 0$ EOS can be well approximated by $E_{sym}^{x=0}(\rho) \approx 32(\rho/\rho_0)^{0.7}$. With $x = -1$, the $E_{sym}^{x=-1}(\rho) \approx 32(\rho/\rho_0)^{1.1}$ is closer to predictions of typical relativistic mean field models [12].

The middle panel shows the proton fraction, x_p , as a function of density, and the top panel gives the mass of a neutron star as a function of the central density. For x_p below 0.14 [34], the direct URCA process does not proceed because energy and momentum conservation cannot be fulfilled. The proton fraction is sensitive to the slope of the symmetry energy [8]. For the $x = -1$ and

$x = -2$ EOSs, the condition for direct URCA is fulfilled for nearly all neutron stars above $1 M_\odot$. For the $x = 0$ EOS, the minimum density for direct URCA is indicated by the vertical dotted line, and the corresponding minimum neutron star mass is indicated by the horizontal dotted line. Neutron stars with masses above $1.39 M_\odot$ will have a central density above the threshold for the direct URCA process.

Isospin diffusion in heavy-ion reactions is the redistribution process of isospin asymmetries carried originally by the colliding partners. The degree and rate of this process depends on the relative pressures of neutrons and protons, namely the slope of the $E_{sym}(\rho)$. It is harder for neutrons and protons to mix up with a stiffer $E_{sym}(\rho)$, leading to a smaller/slower isospin diffusion. Moreover, the distribution of the isospin asymmetry versus density during heavy-ion reactions is completely determined by the $E_{sym}(\rho)$. As an illustration, shown in the insert of Fig. 2 is a snapshot at 20 fm/c of the correlation between the local isospin asymmetry and density in the $^{124}\text{Sn} + ^{124}\text{Sn}$ reaction using the two extreme density dependences of the $E_{sym}(\rho)$. With the very stiff symmetry energy of $x = -2$, a very neutron-rich dilute cloud surrounds a more symmetric denser region up to $1.6\rho_0$. With the very soft symmetry energy of $x = 1$ (it first rises then starts decreasing with the increasing ρ above about $1.3\rho_0$ [25], mimicking one of the results in Ref. [35]), however, the isospin asymmetries at both very low and very high densities are higher than the average asymmetry of the reaction system. The observed inverse relationship between the $\delta(\rho)$ and $E_{sym}(\rho)$ is consistent with the well-known isospin fractionation phenomenon first predicted based on the thermodynamics of asymmetric matter [36, 37]. Similar to neutron skins in heavy nuclei, neutron-rich clouds are dynamically generated in heavy-ion reactions via the isospin diffusion. This indicates that the same underlying physics is at work [20].

In the following, we examine simultaneously the strength of the isospin diffusion and the thickness of neutron skin in ^{208}Pb as a function of the slope parameter $L \equiv 3\rho_0(\partial E_{sym}/\partial \rho)_{\rho_0}$. The degree of isospin diffusion in the reaction of $A+B$ is experimentally measured by using [38]

$$R_i \equiv \frac{2O_I^{A+B} - O_I^{A+A} - O_I^{B+B}}{O_I^{A+A} - O_I^{B+B}}, \quad (2)$$

where O_I is any isospin-sensitive observable. The frequently used ones include the neutron/proton ratio of pre-equilibrium nucleons, ratios of light mirror nuclei and the isospin asymmetry of projectile-like fragments. They all give essentially the same result [18, 39]. By construction, the value of R_i is 1 (-1) for the symmetric $A+A$ ($B+B$) reaction. If a complete isospin equilibrium is reached in the asymmetric reaction $A+B$ as a result of isospin diffusion the value of R_i is about zero. The R_i also has the advantage of reducing significantly its sensitivity to the symmetric part of the EOS. Our calculations

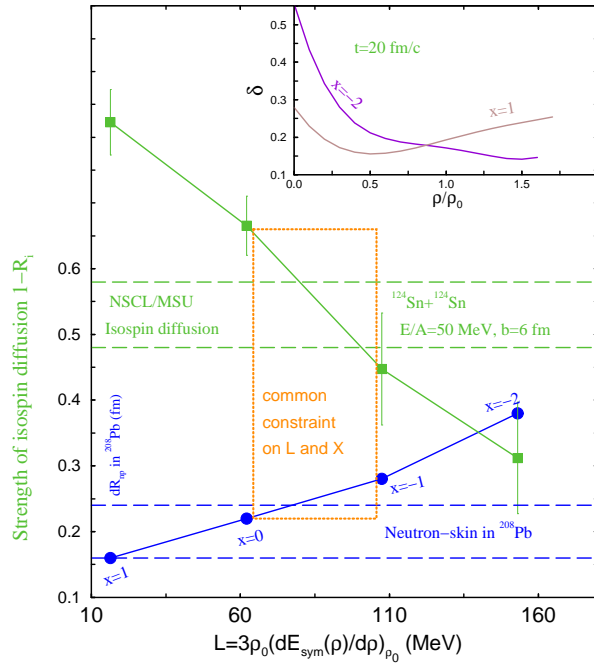


FIG. 2: (Color online) The strength of isospin diffusion in the $^{124}\text{Sn} + ^{112}\text{Sn}$ reaction and the size of neutron skin in ^{208}Pb as a function of the slope of the symmetry energy, respectively. The same EOS is obtained [20]. The strength of isospin diffusion $1 - R_i$ is seen to decrease, while dR_{np} increases with the increasing L as one expects. Taken the fiducial value $dR_{np} = 0.2 \pm 0.04$ fm measured [40] and supported strongly by several recent calculations [12, 23, 24] and the NSCL/MSU data $1 - R_i = 0.525 \pm 0.05$, the $L(X)$ parameter is constrained between 62.1 MeV ($x=0$) and 107.4 MeV ($x=-1$).

are performed using the latest isospin and momentum-dependent transport model using in-medium nucleon-nucleon cross sections consistent with the corresponding single particle potential [21]. Shown in Fig. 2 are the strength of isospin diffusion $1 - R_i$ and the size of neutron skin dR_{np} in ^{208}Pb calculated using the Skyrme Hartree-Fock with interaction parameters adjusted such that the same EOS is obtained [20]. The strength of isospin diffusion $1 - R_i$ is seen to decrease, while dR_{np} increases with the increasing L as one expects. Taken the fiducial value $dR_{np} = 0.2 \pm 0.04$ fm measured [40] and supported strongly by several recent calculations [12, 23, 24] and the NSCL/MSU data $1 - R_i = 0.525 \pm 0.05$, the $L(X)$ parameter is constrained between 62.1 MeV ($x=0$) and 107.4 MeV ($x=-1$).

The corresponding mass vs. radius curves for these EOSs, as well as for APR (using the AV18+ δv +UIX* interaction) are given in Fig. 3. In addition the constraints of causality, the mass-radius relation from estimates of the crustal fraction of the moment of inertia ($\Delta I/I = 0.014$) in the Vela pulsar [41], and the mass-radius relation from the redshift measurement from Ref. [42] are given. Any equation of state should be to the right of the causality line and should cross the other two lines. The hatched regions are the inferred limits on the radius and the radiation radius (the value of the radius which is observed by an observer at infinity) defined as $R_\infty = R/\sqrt{1 - 2GM/Rc^2}$ for a $1.4 M_\odot$ neutron star.

Since all three calculations with $x = 0, -1$ and $x = -2$ have the same compressibility ($K_0 = 211$ MeV), it is clear that the radius is indeed rather sensitive to the sym-

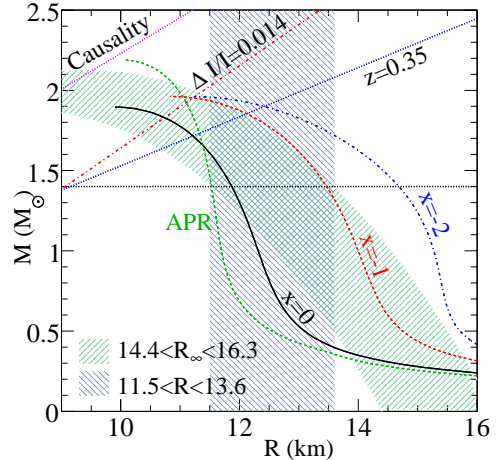


FIG. 3: (Color online) The mass-radius curves for $x = 0, -1$, and -2 and the APR EOS. The limit from causality, the Vela pulsar, and the redshift of EXO0748 are all indicated. The inferred radius of a $1.4 M_\odot$ neutron star and the inferred value of R_∞ are given by the shaded regions.

metry energy while the maximum mass is only slightly modified [8, 43]. The APR EOS has an incompressibility $K_0 = 269$ MeV but almost the same symmetry energy as with $x = 0$. We note that the APR EOS leads to a 16% higher maximum mass ($1.9 M_\odot$ to $2.2 M_\odot$) but only a 5% decrease in radius (12.0 km to 11.5 km) as compared to the results with $x = 0$.

Since only EOSs with symmetry energies between $x = 0$ and $x = -1$ are consistent with the isospin diffusion data and measurements of the skin thickness of lead, we take them as representative of the possible variation in neutron star structure that is consistent with terrestrial nuclear data. Since APR and the $x = 0$ EOS have nearly identical symmetry energies, but slightly different radii, we take the 5% difference as representative of the remaining uncertainty in the symmetric part of the EOS and extend the minimum radius to 11.5 km. Neutron stars with radii larger than 13.6 km are difficult to make without a larger symmetry energy or compressibility [12]. We conclude that only radii between 11.5 and 13.6 km (or radiation radii between 14.4 and 16.3 km) are consistent with the $x = 0$ and $x = -1$ EOSs, and thus consistent with the laboratory data. It is interesting to note that a radius of $R = 12.66$ km was recently predicted for canonical neutron stars using a new effective interaction calibrated by reproducing several collective modes of ^{90}Zr and ^{208}Pb [24]. This radius falls right in the range of our constraints. Moreover, the direct URCA processes is likely for stars with masses larger than $1.39 M_\odot$, which is the limit obtained from the $x = 0$ EOS in Fig. 1.

While estimates of radii based on astrophysical observations are still very challenging, it is useful to compare our results with recent Chandra/XMM-Newton observations. Assuming a mass of $1.4 M_\odot$, the inferred radiation radius, R_∞ , (in km) is 13.5 ± 2.1 [3] or 13.6 ± 0.3 [4]

for the neutron star in ω Cen, 12.8 ± 0.4 in M13 [5], $14.5^{+1.6}_{-1.4}$ for X7 in 47 Tuc [6] and $14.5^{+6.9}_{-3.8}$ in M28 [7], respectively. Except the neutron star in M13 that has a slightly smaller radius, all others fall into our constraints of $14.4 \text{ km} < R_\infty < 16.3 \text{ km}$ within the observational error bars that are still larger than the range we gave in most cases.

Together with more refined observations, future heavy-ion experiments with advanced radioactive beam facilities [44] and measurements of parity violating electron-nucleus scattering [45] will allow us to pin down even more precisely the EOS of neutron rich matter. This

would allow even tighter constraints on neutron star radii. On the other hand, a neutron star radius measurement outside of our prediction may indicate new or non-standard physics.

We would like to thank Dr. Lie-Wen Chen for helpful discussions. The work of B.A. Li was supported in part by the NSF under Grant No. PHY-0354572, PHY0456890 and the NASA-Arkansas Space Grants Consortium Award ASU15154. The work of A.W. Steiner was supported in part by the DOE under grant no. DOE/W-7405-ENG-36.

[1] S.E. Thorsett and D. Chakrabarty, *Astrophys J.* **512**, 288 (1999).

[2] P. Haensel, *A&A* **380**, 186 (2001).

[3] R.E. Rutledge et al., *Astrophys J.* **580**, 413 (2002); *ibid*, **577**, 346 (2002).

[4] B. Gendre, D. Barret and N. A. Webb, *Astron. Astrophys.* **400**, 521 (2003).

[5] B. Gendre, D. Barret and N. Webb, *Astron. Astrophys.* **403**, L11 (2003).

[6] G.B. Rybicki et al., *astro-ph/0506563*.

[7] W. Becker et al., *Astrophys. J.* **594**, 798 (2003).

[8] J.M. Lattimer and M. Prakash, *Phys. Rep.* **333**, 121 (2000); *Astr. Phys. Jour.* **550**, 426 (2001); *Science Vol. 304*, 536 (2004); M. Prakash, J.M. Lattimer, R.F. Sawyer and R.R. Volkas, *Ann. Rev. Nucl. Part. Sci.* **51**, 295 (2001).

[9] D.G. Yakovlev and C.J. Pethick, *Ann. Rev. Astron. Astrophys.* **42**, 169 (2004).

[10] P. Haensel, in “Final Stages of Stellar Evolution”, Eds. J.-M. Hameury and C. Motch, EAS Publications Series (EDP Sciencs, 2003).

[11] H. Heiselberg and V.R. Pandharipande, *Ann. Rev. Nucl. Part. Sci.* **50**, 481 (2000); H. Heiselberg and M. Hjorth-Jensen, *Phys. Rep.* **328**, 237 (2000).

[12] A.W. Steiner, M. Prakash, J.M. Lattimer and P.J. Ellis, *Phys. Rep.* **411**, 325 (2005).

[13] B.A. Li, C.M. Ko and Z. Ren, *Phys. Rev. Lett.* **78**, 1644 (1997); B.A. Li, *ibid* **85**, 4221 (2000); **88**, 192701 (2002).

[14] B.A. Li, C.M. Ko and W. Bauer, topical review, *Int. J. of Modern Phys. E* **7**, 147 (1998); *Isospin Physics in Heavy-Ion Collisions at Intermediate Energies*, Eds. B.A. Li and W. Udo Schröder, Nova Science Publishers, Inc (2001, New York).

[15] P. Danielewicz, R. Lacey and W.G. Lynch, *Science* **298**, 1592 (2002).

[16] V. Baran, M. Colonna, V. Greco and M. Di Toro, *Phys. Rep.* **410**, 335 (2005).

[17] L. Shi and P. Danielewicz, *Phys. Rev. C* **68**, 064604 (2003).

[18] M.B. Tsang et al., *Phys. Rev. Lett.* **92**, 062701 (2004).

[19] L.W. Chen, C.M. Ko and B.A. Li, *Phys. Rev. Lett.* **94**, 032701 (2005).

[20] A.W. Steiner and B.A. Li, *Phys. Rev. C* **72** 041601(R) (2005).

[21] B.A. Li and L.W. Chen, *nucl-th/0508024*, *Phys. Rev. C* (2005) in press.

[22] L.W. Chen, C.M. Ko and B.A. Li, *nucl-th/0509009*, *Phys. Rev. C* (2005) in press.

[23] C.J. Horowitz and J. Piekarewicz, *Phys. Rev. Lett.* **86**, 5647 (2001); *Phys. Rev. C* **66**, 055803 (2002).

[24] B.G. Todd-Rutel and J. Piekarewicz, *Phys. Rev. Lett.* **95**, 122501 (2005).

[25] C.B. Das, S. Das Gupta, C. Gale and B.A. Li, *Phys. Rev. C* **67**, 034611 (2003).

[26] B.A. Li, C.B. Das, S. Das Gupta, C. Gale, *Phys. Rev. C* **69**, 011603(R) (2004); *Nucl. Phys. A* **735**, 563 (2004).

[27] G.M. Welke, M. Prakash, T.T. S. Kuo, S. Das Gupta, and C. Gale, *Phys. Rev. C* **38**, 2101 (1988); C. Gale, G.M. Welke, M. Prakash, S.J. Lee and S. Das Gupta, *ibid* **41**, 1545 (1990).

[28] R.B. Wiringa, *Phys. Rev. C* **38**, 2967 (1988).

[29] J. Zhang, S. Das Gupta and C. Gale, *Phys. Rev. C* **50**, 1617 (1994).

[30] G.W. Hoffmann and W.R. Coker, *Phys. Rev. Lett.* **29**, 227 (1972); P.E. Hodgson, *The Nucleon Optical Model*, pages 613-651, (World Scientific, Singapore, 1994).

[31] J.W. Negele and D. Vautherin, *Nucl. Phys. A* **207**, 298 (1974).

[32] G. Baym, C.J. Pethick, and P. Sutherland, *Astrophys. J.* **170**, 299 (1971).

[33] A. Akmal, V.R. Pandharipande and D.G. Ravenhall, *Phys. Rev. C* **58**, 1804 (1998).

[34] J.M. Lattimer, C.J. Pethick, M. Prakash and P. Haensel, *Phys. Rev. Lett.* **66**, 2701 (1991).

[35] R.B. Wiringa, V. Fiks and A. Fabrocini, *Phys. Rev. C* **38**, 1010 (1988).

[36] H. Müller and B.D. Serot, *Phys. Rev. C* **52**, 2072 (1995).

[37] B.A. Li and C.M. Ko, *Nucl. Phys. A* **618**, 498 (1997).

[38] F. Rami et al., *Phys. Rev. Lett.* **84**, 1120 (2000).

[39] W.G. Lynch, private communications.

[40] V.E. Starodubsky and N.M. Hintz, *Phys. Rev. C* **49**, 2118 (1994); B.C. Clark, L.J. Kerr and S. Hama, *Phys. Rev. C* **67**, 054605 (2003).

[41] B. Link, R. I. Epstein and J.M. Lattimer, *Phys. Rev. Lett.* **83**, 3362 (1999).

[42] J. Cottam, F. Paerels, and M. Mendez, *Nature* **420**, 51 (2002).

[43] M. Prakash, T.L. Ainsworth and J.M. Lattimer, *Phys. Rev. Lett.* **61**, 2518 (1988).

[44] RIA Theory Bluebook, www.oraau.org/ria/RIATG

[45] C.J. Horowitz, S.J. Pollock, P.A. Souder and R. Michaels, *Phys. Rev. C* **63**, 025501 (2001).